BJ www.biochemj.org

BJ Metabolism

Biochem. J. (2012) **441**, 285–296 (Printed in Great Britain) doi:10.1042/BJ20110512

online data

Reduction in BACE1 decreases body weight, protects against diet-induced obesity and enhances insulin sensitivity in mice

Paul J. MEAKIN*[1], Alex J. HARPER†[1,2], D. Lee HAMILTON*, Jennifer GALLAGHER*, Alison D. McNEILLY‡, Laura A. BURGESS*, Lobke M. VAANHOLT§, Kirsten A. BANNON*, Judy LATCHAM†, Ishrut HUSSAIN†[3], John R. SPEAKMAN§, David R. HOWLETT†[4] and Michael L.J. ASHFORD*[5]

*Division of Cardiovascular and Diabetes Medicine, Medical Research Institute, Ninewells Hospital and Medical School, University of Dundee, Dundee DD1 9SY, Scotland, U.K., †Neuroscience Centre of Excellence for Drug Discovery, GlaxoSmithKline R&D, New Frontiers Science Park, Harlow CM19 5AW, U.K., ‡Division of Neuroscience, University of Dundee, Medical Research Institute, Dundee DD1 9SY, Scotland, U.K., and §Aberdeen Centre for Energy Regulation and Obesity, Institute of Biological and Environmental Sciences, University of Aberdeen, Aberdeen AB24 2TZ, Scotland, U.K.

Insulin resistance and impaired glucose homoeostasis are important indicators of Type 2 diabetes and are early risk factors of AD (Alzheimer's disease). An essential feature of AD pathology is the presence of BACE1 (β-site amyloid precursor protein-cleaving enzyme 1), which regulates production of toxic amyloid peptides. However, whether BACE1 also plays a role in glucose homoeostasis is presently unknown. We have used transgenic mice to analyse the effects of loss of BACE1 on body weight, and lipid and glucose homoeostasis. *BACE1*$^{-/-}$ mice are lean, with decreased adiposity, higher energy expenditure, and improved glucose disposal and peripheral insulin sensitivity than wild-type littermates. *BACE1*$^{-/-}$ mice are also protected from diet-induced obesity. BACE1-deficient skeletal muscle and liver exhibit improved insulin sensitivity. In a skeletal muscle cell line, BACE1 inhibition increased glucose uptake and enhanced insulin sensitivity. The loss of BACE1 is associated with increased levels of UCP1 (uncoupling protein 1) in BAT (brown adipose tissue) and UCP2 and UCP3 mRNA in skeletal muscle, indicative of increased uncoupled respiration and metabolic inefficiency. Thus BACE1 levels may play a critical role in glucose and lipid homoeostasis in conditions of chronic nutrient excess. Therefore strategies that ameliorate BACE1 activity may be important novel approaches for the treatment of diabetes.

Key words: β-site amyloid precursor protein-cleaving enzyme 1 (BACE1), glucose uptake, insulin sensitivity, liver, skeletal muscle, uncoupling protein (UCP).

INTRODUCTION

There is a higher risk of sporadic AD (Alzheimer's disease) in patients with Type 2 diabetes and AD patients are more prone to Type 2 diabetes [1,2]. Being obese or overweight in midlife is also implicated as an independent risk factor of AD in later life [3,4]. Furthermore, AD patients exhibit impaired glucose metabolism, hyperinsulinaemia and insulin resistance [5,6], and brains from AD patients display reduced insulin levels, insulin receptor density and signalling [7,8]. AD patients with elevated plasma insulin have reduced CSF (cerebrospinal fluid) insulin levels [5,7] and lower brain glucose utilization [6]. In addition, HFD (high-fat diet) induction of peripheral insulin resistance in an AD transgenic mouse model reduced brain insulin and insulin receptor signalling, and increased AD pathology [9]. Collectively these data indicate that AD is closely associated with insulin resistance, an outcome exacerbated by the presence of Type 2 diabetes and obesity.

A key feature of AD pathology development is the proteolytic cleavage of APP (amyloid precursor protein) by γ- and β-secretase [BACE1 (β-site amyloid precursor protein-cleaving enzyme 1)], which raise levels of Aβs (β-amyloid peptides) that aggregate to form extracellular amyloid plaques [10,11]. Importantly, deletion of BACE1 in APP transgenic mice abolishes neuronal production of Aβ and deposition of amyloid plaques [11–13]. Thus excessive levels and/or activity of BACE1 are thought to be the primary driver for the neurodegeneration and cognitive dysfunction associated with sporadic AD. Indeed, increased BACE1 protein levels and activity have been reported in brains from AD patients [14,15]. Neuronal BACE1 levels and activity increase with age and following pathological events such as oxidative stress, hypoxia and brain injury and are associated with raised Aβ and an increased risk of AD [14–16]. Therefore it is plausible that the insulin resistance and impaired glucose metabolism associated with AD may be connected to raised levels and activity of this enzyme.

BACE1 mRNA is expressed in non-neuronal tissues, although at much lower levels than in the brain [17]. The pancreas is an exception, although the high levels of mRNA comprise three splice variants encoding BACE1 isoforms devoid of β-secretase activity. The presence of BACE1 in skeletal muscle and liver [18,19] raises the possibility that BACE1 activity in

Abbreviations used: Aβ, β-amyloid peptide; AD, Alzheimer's disease; ADDL, Aβ-derived diffusible ligands; AMPK, AMP-activated protein kinase; APP, amyloid precursor protein; BACE1, β-site amyloid precursor protein-cleaving enzyme 1; BAT, brown adipose tissue; DMEM, Dulbecco's modified Eagle's medium; FBS, fetal bovine serum; FFA, free fatty acid; HBS, Hepes-buffered saline; HFD, high-fat diet; IGTT, intraperitoneal glucose tolerance test; ITT, insulin tolerance test; IRS, insulin receptor substrate; OGTT, oral glucose tolerance test; PDK, phosphoinositide-dependent kinase; PKB, protein kinase B; qMR, quantitative magnetic resonance; qRT-PCR, quantitative real-time PCR; RMR, resting metabolic rate; RQ, respiratory quotient; T_4, thyroxine; TG, triacylglycerol; UCP, uncoupling protein; WAT, white adipose tissue; WT, wild-type.

[1] These authors contributed equally to this work.
[2] Present address: Lilly Research Laboratories, Eli Lilly & Co., Erlwood Manor, Sunninghill Road, Windlesham, GU20 6PH. U.K.
[3] Present address: Merck Serono S.A., Chemin des Mines 9, 1202 Geneva, Switzerland
[4] Present address: Wolfson Centre for Age Related Diseases, King's College London, London SE1 1UL, U.K.
[5] To whom correspondence may be addressed (email m.l.j.ashford@dundee.ac.uk).

these tissues may also be up-regulated by stress conditions. *BACE1*-deficient (*BACE1*$^{-/-}$) mice have been reported initially not to show any adverse development, morphology, physiology or gross behaviour [11–13]. However, later studies indicated subtle behavioural changes with mild impairments in spatial learning and memory [20], or a more timid and anxious phenotype were reported [21]. Despite the link between AD, insulin resistance and glucose homoeostasis deregulation in humans and rodents, the involvement of BACE1 in whole-body glucose and energy homoeostasis has not been investigated. In the present paper we show that mice lacking BACE1 are lean, resistant to diet-induced obesity, and display increased peripheral tissue insulin sensitivity with improved whole-body glucose disposal. These results delineate a novel aspect of BACE1 function in metabolic homoeostasis and provide a possible functional link between the levels of this key amyloid processing enzyme and the reciprocal connection between AD and Type 2 diabetes.

MATERIALS AND METHODS

Animals

BACE1$^{-/-}$ mice were obtained from GlaxoSmithKline and were continued on the C57Bl6/J background, providing *BACE1*$^{-/-}$ and *BACE1*$^{+/-}$ mice and WT (wild-type) littermates. Mice were maintained on a 12 h light/dark cycle with free access to water and standard rodent chow [7.5 % fat, 75 % carbohydrate and 17.5 % protein by energy (RM1 diet); Special Diet Services], except where noted, and were housed singly in specific pathogen-free barrier facilities. Genotyping of mice was performed by PCR amplification of ear DNA with primers as described previously [21]. All animal care protocols and procedures were performed in accordance to the Animal Scientific Procedures Act (1986) and with approval of the University of Dundee Animal Ethics Committee. *BACE1*$^{-/-}$ and *BACE1*$^{+/-}$ mice were studied with appropriate age-matched littermate controls. For assessment of fat and lean mass, a magnetic resonance analyser was used (Echo Medical Systems). For HFD studies, mice were fed with chow containing, by energy, 45 % fat, 20 % protein and 35 % carbohydrate (catalogue number 58V8, TestDiet®, Purina Mills) for the indicated number of weeks. Mice were weighed weekly and food intake was measured over a 3-day period each week. Feed efficiency was calculated as grams of weight gained per grams of food consumed. To assess locomotor activity, mice were habituated to the test room and chamber for 5 days prior to testing to minimize any stress-induced changes in activity. Spontaneous locomotor activity was measured using an activity monitor (AM1051 Activity Monitor, Benwick Electronics) consisting of a Perspex chamber (32 cm × 20 cm × 19 cm) positioned within a frame equipped with IR beams along its length and width. Locomotor activity was recorded automatically by counting the number of beam breaks in the test period. A mouse was considered mobile if there were two consecutive beam breaks but not if the same beam was broken twice. Total beam breaks were recorded in 5 min time-bins over a period of 15 min. The results represent the accumulative activity over the total 15 min test period.

Physiological measurements

Nose-to-anus length was measured either post-mortem or in anaesthetized mice, with the observer blinded to the genotype. Blood samples were collected from mice via tail vein bleeds or from cardiac puncture performed on terminally anaesthetized mice. Blood glucose was measured using a glucometer (Ascensia). Plasma insulin, leptin, T_4 (thyroxine), adiponectin and corticosterone levels were measured using mouse insulin (Linco), leptin and T_4 (Alpha Diagnostic), adiponectin (R&D Systems) and corticosterone (Enzo Life Sciences) ELISA kits. Colorimetric assays were used to measure plasma FFA (free fatty acid; Roche) and cholesterol (Biovision) with TG (triacylglycerol 'triglyceride') measured using a Triglyceride Determination kit (Sigma). Lipids were extracted from 0.3–0.5 g of pooled mouse faeces by homogenizing in 20 volumes of chloroform/methanol [2:1 (v/v)] in an Ultra Turrax tissue disrupter (Fisher Scientific). Total lipids were prepared according to the Folch method [22] and non-lipid impurities removed by washing with 0.88 % KCl. The weight of lipids was determined gravimetrically after evaporation of solvent and overnight desiccation under vacuum. Glucose tolerance tests were performed on mice after a 16 h overnight fast. Animals were injected intraperitoneally with D-glucose (2.0 or 1.0 g/kg of body weight) or given D-glucose (3 mg/kg of body weight) orally and blood glucose levels determined by glucometer. Insulin tolerance tests were carried out on mice after a 4 h fast by intraperitoneal injection of 0.75 unit of human insulin/kg of body weight (Actrapid®, Novo Nordisk) and blood glucose levels were determined as above. RMR (resting metabolic rate) was measured at a thermoneutral temperature (30 °C) by indirect open-flow respirometry system (Xentra 1400, Servomex) as described previously [23]. RQ (respiratory quotient) was determined from the ratio of the rates of oxygen consumption and carbon dioxide production. Quantitative determination of Aβ levels (A$\beta_{x\text{-}40}$ and A$\beta_{x\text{-}42}$) was performed using the appropriate [human/rat (mouse) β-amyloid] ELISA kits (Wako). BACE1 activity was determined using a quenched fluorescence assay as follows. A portion (25 μg) of tissue lysate was added to 50 μl of assay buffer [0.1M sodium acetate (pH 4)] and 10 μM BACE1 synthetic peptide substrate (β-secretase substrate IV fluorogenic, Calbiochem), based on the β-secretase cleavage site of the APP Swedish mutation, in a 96-well plate. The reaction was incubated at 37 °C in the dark and the fluorescence (excitation wavelength = 350 nm and emission wavelength = 495 nm) was measured after 1 h. Background activity was subtracted and results are expressed as RFUs (relative fluorescent units).

Cell culture

C2C12 mouse myoblast cells were grown in DMEM (Dulbecco's modified Eagle's medium, Sigma) supplemented with 10 % FBS (fetal bovine serum), and 1 % penicillin and streptomycin at 37 °C in a humidified atmosphere of 95 % air and 5 % CO_2. C2C12 cells were plated at 200000 cells per well on six-well plates in growth medium [high-glucose DMEM (Invitrogen), 10 % (v/v) FBS (Sera Labs) and 1 % (v/v) penicillin and streptomycin (Gibco)]. The following day cells were moved to differentiation medium [high-glucose DMEM (Invitrogen), 2 % (v/v) horse serum (Invitrogen) and 1 % (v/v) penicillin and streptomycin (Gibco)] and allowed to differentiate for 5 days before treatment. For transfection, cells were plated on to 10-cm plates at 500000 cells per plate and transfected with 10 μg of plasmid DNA of either empty vector (pcDNA3.1) or pcDNA3.1 containing full-length BACE1 using Lipofectamine™ 2000 reagent (Invitrogen), according to the manufacturer's instructions. Cells were selected for 5 days with 1 mg/ml G418 (Sigma–Aldrich), and then plated and differentiated as described above. For BACE1-inhibitor treatments, cells were differentiated as described for 4 days and treated with Merck-3 (50 nM β-Secretase Inhibitor IV, Calbiochem) overnight. Cells were then treated as described above.

Glucose uptake assays

C2C12 myotubes were serum-starved for 2 h followed by insulin stimulation (100 nM) for 30 min. Insulin-stimulated glucose

uptake was determined as follows: C2C12 myotubes were washed twice with HBS [(Hepes-buffered saline); 140 mM NaCl, 20 mM Hepes, 5 mM KCl, 2.5 mM $MgSO_4$ and 1 mM $CaCl_2$ (pH 7.4)] and incubated for 10 min in HBS containing 10 μM 2-deoxy-D-[^{3}H]glucose (1 μCi/ml, PerkinElmer) at room temperature (20 °C). Non-specific uptake was determined by quantifying cell-associated radioactivity in the presence of 10 μM cytochalasin B (Sigma–Aldrich). Medium was aspirated and adherent cells were washed twice with ice-cold 0.9 % NaCl. Cells were subsequently lysed in 50 mM NaOH and cell-associated radioactivity was quantified using a Beckman LS 6000IC scintillation counter.

Immunoprecipitation and Western blotting

After an overnight fast, mice were injected with 2 units of insulin/kg of body weight (unless otherwise stated), or an equal volume of saline, intraperitoneally. Tissues (quadriceps muscle, liver and perigenital fat) were collected in liquid nitrogen, 5, 6 and 7 min after injection respectively. C2C12 cells, grown in six-well plates, were exposed to 50 nM Merck-3 or vehicle for 24 h, prior to incubation with insulin (5 nM) or vehicle for 30 min. Tissue or cell samples were homogenized in lysis buffer, and protein isolation, content, immunoblotting and analysis were performed as described previously [24]. Primary antibodies used were: anti-BACE1 (Calbiochem or Sigma; 1:1000 dilution), anti-[phospho-PKB (protein kinase B) (Ser^{473})], anti-[phospho-IRS (insulin receptor substrate) 1 (Tyr^{612})], anti-(total PKB) and anti-IRS1 (Cell Signaling Technology; 1:1000 dilution), anti-[UCP (uncoupling protein) 1] (Abcam; 1:1000 dilution), and anti-BACE2 (R&D Systems; 1:1000 dilution), anti-tubulin (Sigma; 1:1000 dilution) and anti-(β-actin) (Sigma; 1:10 000 dilution).

qRT-PCR (quantitative real-time PCR)

Gene expression was determined by qRT-PCR using TaqMan®. Total RNA was extracted from frozen tissue using the TRISOL method (Sigma). A portion (1 μg) of total RNA was used for first-strand cDNA synthesis using Superscript II (Invitrogen). For quantitative PCR, 1.25 ng of cDNA was amplified (Prism 7700), using assay-on-demand premixed (Applied Biosystems) TaqMan® primers and probes [UCP1 (Mm01244861_m1); UCP2 (Mm00627597_m1); and UCP3 (Mm00494077_m1)]. Genes of interest were normalized to actin (Mm00607929_s1) as a control gene and are expressed relative to gene expression in the control group.

Statistics

Comparisons between groups were made using unpaired or paired two-tailed Student's *t* test, one sample Student's *t* test, ANCOVA (analysis of co-variance) or ANOVA with repeated measures and Bonferroni post-test analysis as appropriate. Results are means $\pm$ S.E.M. P values $\leqslant 0.05$ were considered statistically significant.

RESULTS

BACE1$^{-/-}$ mice have decreased body weight and adiposity

We used *BACE1*$^{-/-}$ mice produced by targeted deletion of most of the first coding exon [21]. BACE1 protein was absent in the cerebral cortex, skeletal muscle and liver of *BACE1*$^{-/-}$ mice, whereas heterozygote BACE1 mouse (*BACE1*$^{+/-}$) tissues expressed half the amount of BACE1 as tissue from WT littermates (Figure 1A). BACE1 protein exhibits a single band at molecular mass of $\sim$70 kDa, indicative of the mature (glycosylated) form of the protein [16]. To show that loss of BACE1 resulted in a functional reduction in APP cleavage, levels of Aβ were measured in WT and *BACE1*$^{-/-}$ mice cerebral cortices. The amounts of A$\beta_{x\text{-}40}$ and A$\beta_{x\text{-}42}$, the main enzymatically processed forms of Aβ [10,15,16], were reduced significantly in the *BACE1*$^{-/-}$ mice cortex compared with WT controls (Figure 1B). The remaining Aβ peptides observed in the *BACE1*$^{-/-}$ mice cortex are probably derived from BACE2 activity, which is present in glial cells [25] and is detectable in *BACE1*$^{-/-}$ mice cortex samples (Figure 1B), or other aspartic protease activity present in the tissue. In our hands, *BACE1*$^{-/-}$ mice are viable and fertile, and lived longer than 21 months without overt signs of any abnormalities. No gross or histological differences were detected in the brain, muscle, liver, heart or pancreas of *BACE1*$^{-/-}$ mice (results not shown). *BACE1*$^{-/-}$ mice (6–8 weeks old) fed a regular chow diet were significantly lighter than their WT littermates. This weight difference was maintained during growth for male and female *BACE1*$^{-/-}$ mice (Figures 1C and 1D) and at 1 year of age they weighed 18 % ($P = 0.004$) and 16 % ($P < 0.001$) less respectively than their WT littermates. The average length of *BACE1*$^{-/-}$ mice was unaltered compared with their WT littermates (Figure 1E). Although no evidence of sexual dimorphism was observed, we focused our research predominantly on male mice. *BACE1*$^{+/-}$ mice did not exhibit any difference in body mass at 10 weeks of age or when body mass was followed for an additional 24 weeks compared with their WT littermates (Supplementary Figure S1A at http://www.BiochemJ.org/bj/441/bj4410285add.htm).

BACE1$^{-/-}$ mice had reduced relative amounts of perigenital fat compared with their WT littermates (Supplementary Figure S1B), and qMR (quantitative magnetic resonance) scanning revealed they had decreased total body fat (Figure 1F). *BACE1*$^{-/-}$ mice exhibited elevated heart and brain mass, but normal liver and reduced BAT (brown adipose tissue) mass, relative to their total body mass (Supplementary Figures S1C–S1F). Consistent with their reduced body fat, *BACE1*$^{-/-}$ mice had decreased (46 % lower) serum leptin (Figure 1G), although they displayed no difference in serum levels of FFA, TG or cholesterol compared with WT mice (Table 1). These results indicate that the reduced body mass of *BACE1*$^{-/-}$ mice is due to decreased lipid content. Cumulative food intake of *BACE1*$^{-/-}$ mice was unchanged compared with their WT littermates (Figure 2A), whereas relative food intake was significantly higher (Figure 2B). This resulted in an overall reduced feed efficiency in *BACE1*$^{-/-}$ mice compared with WT controls (Figure 2C). Although the mean mass of faeces was unchanged between *BACE1*$^{-/-}$ mice and littermate controls (Figure 2D), the lipid content of faeces from *BACE1*$^{-/-}$ mice was reduced significantly (Figure 2E). Indirect calorimetry showed that *BACE1*$^{-/-}$ mice had a higher RMR than WT mice (Figure 2F), $\sim$7 % more than expected for their body mass and sex, and this was accompanied (Figure 2G) by an increased RQ. We were unable to detect a difference in locomotor activity between *BACE1*$^{-/-}$, *BACE1*$^{+/-}$ and WT mice (Figure 2H). Plasma levels of T_4 were unchanged in *BACE1*$^{-/-}$ mice (Table 1).

BACE1$^{-/-}$ mice have improved glucose disposal and increased insulin sensitivity

Fasting blood glucose levels were unaltered in *BACE1*$^{-/-}$ mice, whereas *ad libitum*-fed blood glucose levels were significantly lower than that of their WT littermates (Figure 3A). Fasting plasma insulin levels were also unchanged (Table 1). IGTTs (intraperitoneal glucose tolerance tests) showed that *BACE1*$^{-/-}$

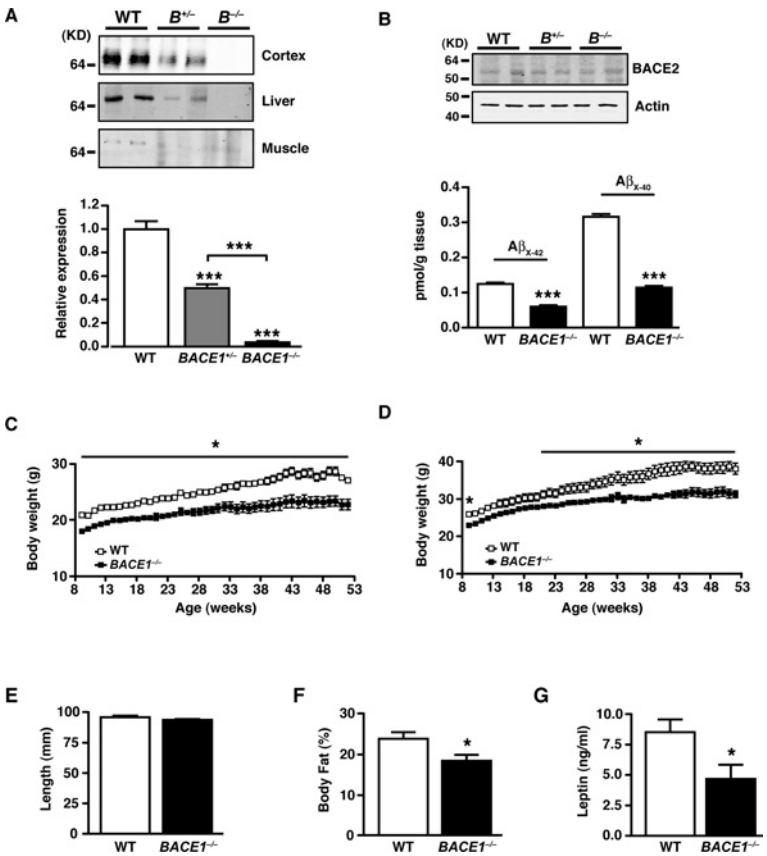

Figure 1 BACE1$^{-/-}$ mice exhibit reduced adiposity

(**A**) BACE1 protein levels in *BACE1*$^{-/-}$, *BACE1*$^{+/-}$ and WT mice, as shown by representative immunoblots of mouse cerebral cortex, skeletal muscle and liver. The histogram (bottom panel) shows mean normalized levels of BACE1 in cortex from WT, *BACE1*$^{+/-}$ and *BACE1*$^{-/-}$ mice following 20 weeks fed on the regular chow diet. WT, $n = 11$; *BACE1*$^{+/-}$, $n = 11$; *BACE1*$^{-/-}$, $n = 12$. (**B**) Representative immunoblots of BACE2 in WT, *BACE1*$^{+/-}$ and *BACE1*$^{-/-}$ mouse cerebral cortices. The histogram (bottom panel) shows levels of A$\beta_{x\text{-}42}$ and A$\beta_{x\text{-}40}$ in the cerebral cortex of WT and *BACE1*$^{-/-}$ mice. WT, $n = 5$; *BACE1*$^{-/-}$, $n = 6$. Molecular mass is given in kDa on the left-hand side. Male (**C**) and female (**D**) body mass curves of age-matched WT littermate and *BACE1*$^{-/-}$ mice fed on a regular chow diet, monitored over a period of 45 weeks from 9 weeks of age. The results in (**C**) and (**D**) are means ± S.E.M. from 9–12 animals of each genotype. (**E**) Male *BACE1*$^{-/-}$ mice have unaltered body length compared with the WT controls. WT, $n = 20$; *BACE1*$^{-/-}$, $n = 19$. (**F**) Percentage body fat determined by qMR imaging in 8-month-old male WT and *BACE1*$^{-/-}$ mice. WT, $n = 5$; *BACE1*$^{-/-}$, $n = 7$. (**G**) Fasting blood leptin levels in 8-month-old male mice of the indicated genotypes. WT, $n = 12$; *BACE1*$^{-/-}$, $n = 15$. Results are means ± S.E.M. $^{*}P < 0.05$; $^{**}P < 0.01$; $^{***}P < 0.001$.

Table 1 Metabolic characteristics of WT and *BACE1*$^{-/-}$ mice fed either a regular chow or an HFD

Male *BACE1*$^{-/-}$ or WT mice were fed on regular chow or an HFD *ad libitum*. Serum was collected from fasted 8-month-old mice, and the indicated metabolic parameters measured. Results are means-± S.E.M. from measurements obtained from 7–13 animals per group.

		WT		*BACE1*$^{-/-}$	
Parameter	Diet...	Regular	High fat	Regular	High fat
Serum insulin (pg/ml)		277 ± 23	1056 ± 179*	267 ± 20	414 ± 72*†
Serum adiponectin (μg/ml)		9.93 ± 0.57	11.05 ± 1.22	10.87 ± 0.86	10.02 ± 0.60
Serum cholesterol (ng/ml)		4.86 ± 0.21	8.48 ± 0.48*	4.75 ± 0.19	7.65 ± 0.28*
Serum FFA (mM)		0.31 ± 0.03	0.36 ± 0.06	0.28 ± 0.03	0.29 ± 0.02
Serum TG (mM)		1.21 ± 0.14	1.28 ± 0.12	1.26 ± 0.12	1.35 ± 0.07
Serum T_4 (μg/dl)		8.44 ± 0.35	7.75 ± 0.49	7.62 ± 0.25	7.70 ± 0.78
Serum corticosterone (ng/ml)		68.2 ± 11.8	55.8 ± 8.1	111.5 ± 22.4	94.1 ± 7.1 †

$^{*}P < 0.05$ compared with regular chow.
$^{\dagger}P < 0.05$ compared with corresponding WT.

mice had increased glucose clearance from the peripheral circulation compared with their WT littermates (Figures 3B and 3C). One-year-old *BACE1*$^{-/-}$ mice also had increased glucose disposal following OGTTs (oral glucose tolerance tests) in comparison with age-matched WT controls (Figures 3D and 3E). *BACE1*$^{+/-}$ mice, despite fasting and fed glucose levels equivalent to WT controls (Supplementary Figures S2A and S2B at http://www.BiochemJ.org/bj/441/bj4410285add.htm), also exhibited increased glucose disposal (Figures 3B and 3C). *BACE1*$^{-/-}$, but not *BACE1*$^{+/-}$, mice showed a significantly greater decrease in blood glucose during ITTs (insulin tolerance tests) at all of the time points examined (Figure 3F). Thus

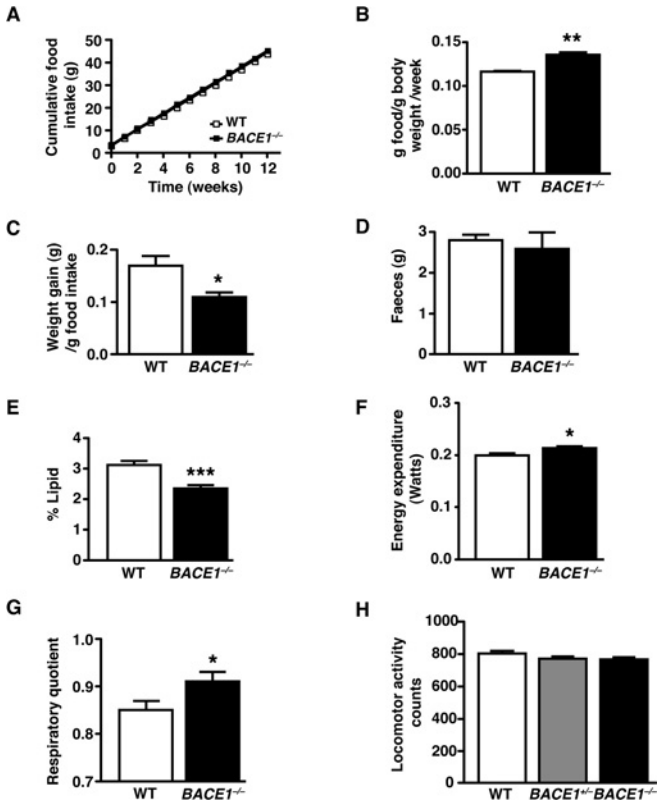

Figure 2 *BACE1*$^{-/-}$ mice have increased relative food intake and energy expenditure

(**A**) Cumulative food intake, measured over 12 weeks, in 3-month-old male mice of the indicated genotypes. (**B**) Food intake per mouse per week normalized by body mass (relative food intake). (**C**) *BACE1*$^{-/-}$ mice have decreased feed efficiency compared with the WT controls. Results in (**A**–**C**) are from 5–7 animals of each genotype. (**D**) Mean mass of faeces over 24 h for WT and *BACE1*$^{-/-}$ mice. (**E**) Lipid content of faeces in WT and *BACE1*$^{-/-}$ mice. Results in (**D**) and (**E**) are from seven animals of each genotype. (**F**) Energy expenditure determined by indirect calorimetry in 8-month-old WT and *BACE1*$^{-/-}$ mice. (**G**), *BACE1*$^{-/-}$ mice have an increased RQ compared with the WT mice. Results in (**F**) and (**G**), WT, $n = 14$ and *BACE1*$^{-/-}$, $n = 12$. (**H**) Effect of genotype on locomotor activity. WT, $n = 9$; *BACE1*$^{+/-}$, $n = 10$; *BACE1*$^{-/-}$, $n = 6$. Results are means $\pm$ S.E.M. $^{*}P < 0.05$; $^{**}P < 0.01$; $^{***}P < 0.001$.

BACE1$^{-/-}$ mice have increased whole-body insulin sensitivity in comparison with their littermate controls.

BACE1$^{-/-}$ mice are protected from HFD-induced obesity and insulin resistance

When *BACE1*$^{-/-}$ mice were challenged for 20 weeks with an HFD (45 % of total calories derived from fat), mass accumulation was significantly reduced compared with age-matched WT controls (Figure 4A). The relative increase in body mass at the end of the HFD was 49.8 % and 31.4 % for WT and *BACE1*$^{-/-}$ mice respectively. Indeed the final masses of *BACE1*$^{-/-}$ mice after the HFD were comparable with age-matched WT mice on a regular chow diet (mass of HFD-fed BACE$^{-/-}$ mice $= 32.7 \pm 1.2$ g, mass of regular-chow-diet-fed WT mice $= 31.6 \pm 0.5$ g). Cumulative food intake was slightly less for HFD-fed *BACE1*$^{-/-}$ mice (Figure 4B), although relative food intake was increased and feed efficiency decreased compared with WT mice (Supplementary Figures S2E and S2F). qMR analysis confirmed that the fat mass of HFD-fed *BACE1*$^{-/-}$ mice, although increased ($P < 0.01$) relative to age-matched

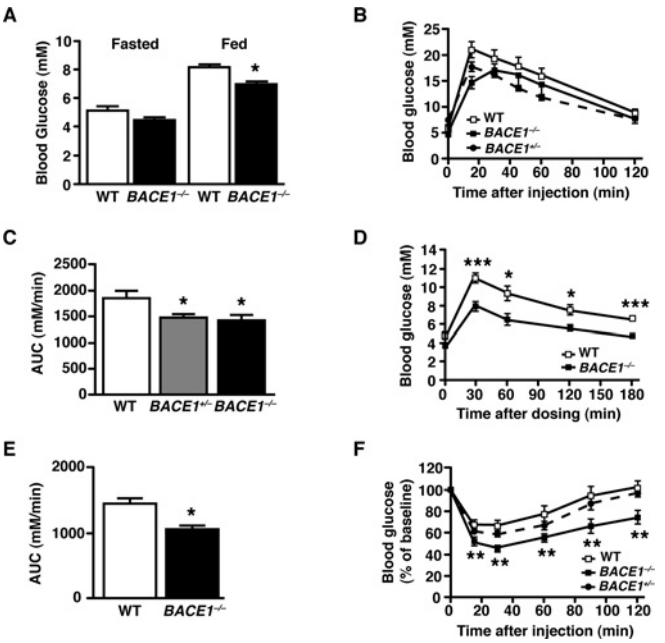

Figure 3 Improved insulin sensitivity and glucose homoeostasis in *BACE1*$^{-/-}$ mice

(**A**) Fasted and fed blood glucose levels in 8-month-old male mice of the indicated genotypes ($n = 11$–18). (**B**) IGTTs were performed on 8-month-old male mice of the indicated genotypes ($n = 10$–12). (**C**) Quantification of the AUC (area under the curve) for the total glycaemic excursions shown in (**B**). (**D**) OGTT in 12-month-old male WT and *BACE1*$^{-/-}$ mice with quantification of the total glycaemic excursion shown in (**E**). WT, $n = 11$; *BACE1*$^{-/-}$, $n = 9$. (**F**) ITT for 8-month-old male mice of the indicated genotypes ($n = 12$–17). Results are means $\pm$ S.E.M. $^{*}P < 0.05$; $^{**}P < 0.01$; $^{***}P < 0.001$.

BACE1$^{-/-}$ mice on a regular chow diet, was significantly reduced compared with HFD-fed WT littermates (Figure 4C). Although leptin levels increased ($P < 0.001$; compared with the results shown in Figure 1G) in WT and *BACE1*$^{-/-}$ mice following the HFD, *BACE1*$^{-/-}$ leptin levels were 60 % lower than WT mice (Figure 4D), as expected from their reduced adiposity. Thus BACE1 contributes to body mass regulation in mice and the absence of this protein provides protection against excessive weight gain on an HFD.

A high proportion of C57Bl6/J mice fed on an HFD go on to display obesity-induced impairment of glucose homoeostasis and insulin resistance [26]. Indeed, the HFD significantly increased fasted and fed blood glucose concentrations in WT and *BACE1*$^{-/-}$ mice compared with their regular-chow-fed counterparts, although *BACE1*$^{-/-}$ mice maintained significantly lower glucose levels than WT littermates under both conditions (Figure 4E). The levels of serum FFAs and TG were unchanged in WT and *BACE1*$^{-/-}$ mice, although cholesterol levels were increased in both groups on the HFD (Table 1). HFD-fed WT mice showed a 4.5-fold increase in serum insulin concentrations, whereas *BACE1*$^{-/-}$ mice, despite having an identical serum insulin level to WT mice fed on regular chow, displayed less than a 2-fold increase (Table 1). Consistent with these results, HFD-fed WT mice exhibited impaired glucose disposal compared with regular-chow-fed WT mice, whereas HFD-fed *BACE1*$^{-/-}$ mice cleared glucose from the peripheral circulation significantly better than the HFD-fed WT controls (Figures 4F and 4G). The HFD-fed *BACE1*$^{-/-}$ mice also maintained a higher insulin sensitivity compared with their WT littermates (Figure 4H). Corticosterone levels were similar for WT and *BACE1*$^{-/-}$ mice fed on the regular chow diet and were raised for both genotypes following the HFD,

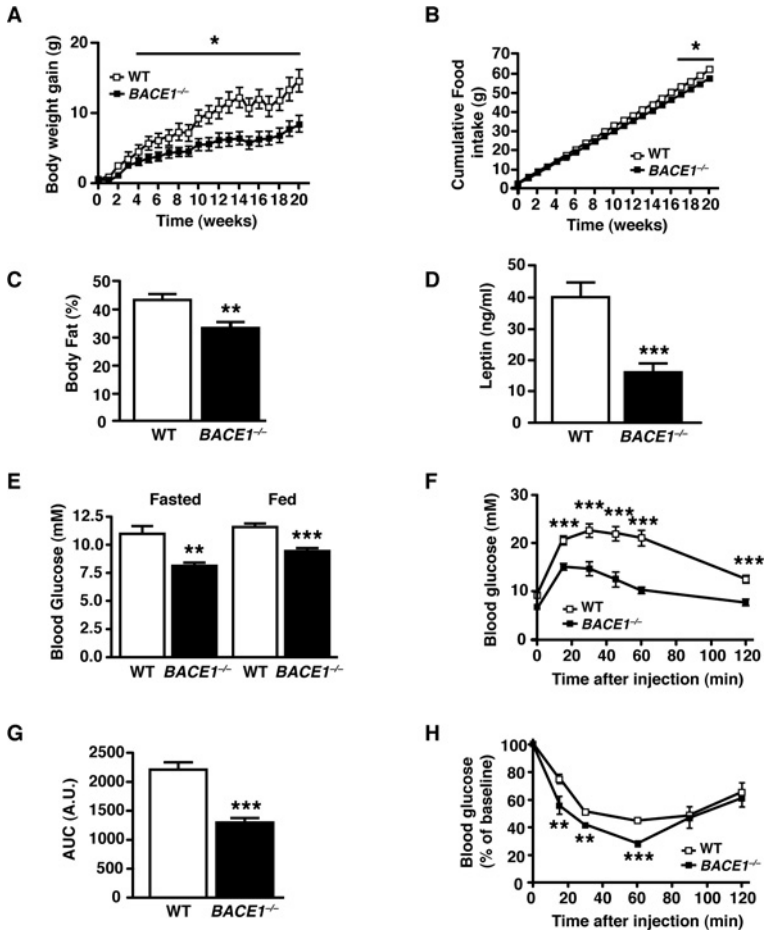

Figure 4 HFD-fed *BACE1*$^{-/-}$ mice are less susceptible to weight gain and loss of glucose homoeostasis

(**A**) Body mass gain of age-matched male WT littermate and *BACE1*$^{-/-}$ mice fed on an HFD, monitored over a period of 20 weeks from 5 months-of-age. (**B**) Cumulative food intake, measured over 20 weeks, of age-matched male WT littermate and *BACE1*$^{-/-}$ mice fed on an HFD. Results in (**A**) and (**B**) are means ± S.E.M. from 6–11 animals of each genotype. (**C**) The percentage body fat determined by qMR imaging in 10-month-old male WT and *BACE1*$^{-/-}$ mice following 20 weeks of the HFD. WT, $n = 7$; *BACE1*$^{-/-}$, $n = 11$. (**D**) Fasting blood leptin levels in 10-month-old male mice of the indicated genotypes, following 20 weeks of a HFD. WT, $n = 11$; *BACE1*$^{-/-}$, $n = 11$. (**E**) Fasting and fed blood glucose levels in 8-month-old male mice of the indicated genotypes, following 20 weeks on a HFD ($n = 7$–11). (**F**) IGTTs were performed on 8-month-old male mice of the indicated genotypes following 20 weeks of the HFD. WT, $n = 7$; *BACE1*$^{-/-}$, $n = 5$ (**G**) Quantification of the AUC (area under the curve) for the total glycaemic excursions shown in (**F**). (**H**) ITTs for 8-month-old male mice of the indicated genotypes, following 20 weeks of an HFD. WT, $n = 7$; *BACE1*$^{-/-}$, $n = 5$. Results are means ± S.E.M. $^{*}P < 0.05$; $^{**}P < 0.01$; $^{***}P < 0.001$.

with the increase showing significance only for the *BACE1*$^{-/-}$ mice (Table 1).

BACE1$^{+/-}$ mice exhibit time-dependent resistance to diet-induced obesity

BACE1$^{+/-}$ mice fed on the HFD initially exhibited resistance to mass gain (Figure 5A), but by the end of the HFD period there was no significant difference in their mean body mice compared with the HFD-fed WT controls (mass of the *BACE1*$^{+/-}$ mass = 42.8 ± 2.6 g, mass of the WT mice = 46.2 ± 0.5 g; $P > 0.05$). Thus *BACE1*$^{+/-}$ mice, although initially comparatively resistant to mass gain when fed on the HFD, eventually exhibit the same level of adiposity as WT mice. In addition, although *BACE1*$^{+/-}$ mice after 10 weeks of being fed on the HFD displayed better glucose disposal and insulin sensitivity (Figures 5C and 5D) compared with their HFD-fed WT counterparts, these metabolic improvements were attenuated by the end of the HFD period (Figures 5E and 5F). Indeed, the 20-week HFD-fed *BACE1*$^{+/-}$ mice demonstrated a non-significant trend to lower fasted, but did exhibit reduced fed, blood glucose levels compared with the HFD-fed WT controls (Supplementary Figures S2C and S2D). These time-dependent changes in adiposity and glucose homoeostasis during the HFD were observed for *BACE1*$^{+/-}$ mice, and not *BACE1*$^{-/-}$ mice. This raised the possibility that dietary fat content influences BACE1 levels and/or activity in peripheral tissues. In support of this hypothesis, a 20-week HFD was shown to increase BACE1 protein levels in skeletal muscle of WT and *BACE1*$^{+/-}$ mice (Figure 5F) and to increased levels of A$\beta_{x\text{-}42}$ (but not A$\beta_{x\text{-}40}$; results not shown) in the cerebral cortex of WT mice, but not *BACE1*$^{-/-}$ mice (Supplementary Figure S3 at http://www.BiochemJ.org/bj/441/bj4410285add.htm). However, the low levels of Aβ in control peripheral tissues precluded the use of the Aβ assay to monitor BACE1 activity. Thus we determined BACE1 activity directly using a quenched fluorescence assay and demonstrated that BACE1 protease activity in skeletal muscle and liver of WT and *BACE1*$^{+/-}$ mice was significantly increased by the HFD, compared with BACE1 activity in tissues of age-matched regular-chow-fed WT and *BACE1*$^{+/-}$ mice (Figure 5G and 5H).

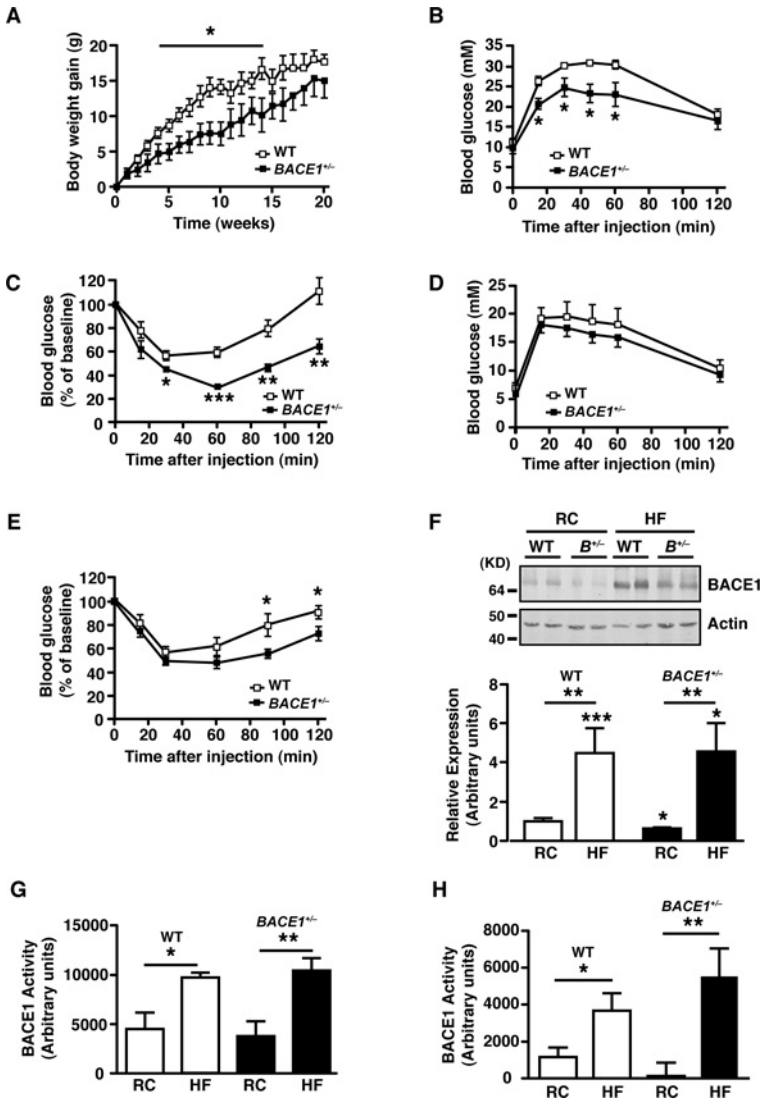

Figure 5 ***BACE1*$^{+/-}$ mice show time-limited resistance to an HFD**

(**A**) Body mass gain of age-matched male WT littermate and *BACE1*$^{+/-}$ mice fed on an HFD, monitored over a period of 20 weeks from 3 months of age. Note that $P < 0.05$ for weeks 4–14 only. WT, $n = 8$; *BACE1*$^{+/-}$, $n = 7$. IGTT (**B**) and ITT (**C**) for WT and *BACE1*$^{+/-}$ mice, after 10 weeks on an HFD. IGTT (**D**) and ITT (**E**) for WT and *BACE1*$^{+/-}$ mice, after 20 weeks on an HFD. WT, $n = 8$; *BACE1*$^{+/-}$, $n = 7$ for (**B**)–(**E**). (**F**) Representative immunoblots of BACE1 in skeletal muscle of male WT and *BACE1*$^{+/-}$ mice following 20 weeks on the regular chow (RC) diet or the HFD. The histogram shows mean normalized levels of BACE1 in skeletal muscle ($n = 9$–15). Molecular mass is given in kDa on the left-hand side. BACE1 activity for skeletal muscle (**G**) and liver (**H**) of WT and *BACE1*$^{+/-}$ mice following 20 weeks on the regular chow diet or the HFD ($n = 6$–11). Results are means ± S.E.M. $^{*}P < 0.05$; $^{**}P < 0.01$; $^{***}P < 0.001$.

BACE1 reduction increases the insulin sensitivity of liver and skeletal muscle, and increases glucose uptake in C2C12 cells

The results from the ITTs indicated that BACE1 influences the insulin signalling pathway in tissues responsible for peripheral glucose clearance. To assess insulin signalling strength we measured phospho-PKB levels in skeletal muscle and liver following intraperitoneal injection of insulin (2 units/kg of body weight). In the basal state, phospho-PKB levels were unchanged in *BACE1*$^{-/-}$ and *BACE1*$^{+/-}$ mice compared with the WT controls. However, in response to insulin stimulation, *BACE1*$^{-/-}$ and *BACE1*$^{+/-}$ mice displayed increased phospho-PKB levels in skeletal muscle and liver compared with their WT littermates (Figure 6). Thus removal or reduction in BACE1 increases insulin signalling in skeletal muscle and liver *in vivo*. Total PKB levels were unchanged in insulin-stimulated or unstimulated muscle and liver of *BACE1*$^{-/-}$ and *BACE1*$^{+/-}$ mice in comparison with WT tissues (Figure 6). To demonstrate that altered insulin sensitivity is directly associated with reduced BACE1 activity we used the cell-permeant BACE1 inhibitor Merck-3 [27] to treat the mouse skeletal muscle cell line C2C12. C2C12 cells express BACE1, exhibiting a single band of ~70 kDa (Figure 7A). Merck-3 has an IC_{50} value of ~30 nM to inhibit the cleavage of APP in cells [28]. C2C12 cells, in the absence and presence of 50 nM Merck-3, were stimulated with 5 nM insulin and phospho-PKB levels monitored. Merck-3, in the absence of insulin, had no effect on phospho-PKB, whereas insulin-stimulated phospho-PKB was enhanced in cells treated with Merck-3 (Figure 7B). Merck-3 had no effect on total PKB levels in these cells (Figure 7B). To examine whether the increased phospho-PKB reflected increased insulin receptor kinase activity, the tyrosine phosphorylation of IRS-1 (phospho-IRS-1) in insulin-stimulated C2C12 cells was

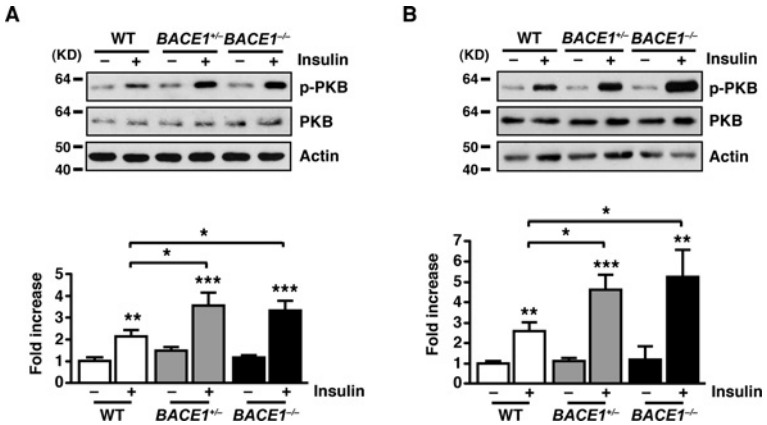

Figure 6 Increased PKB phosphorylation by insulin in muscle and liver BACE1 $^{-/-}$ mice

Representative immunoblots of insulin-stimulated phosphorylation of PKB at Ser^{473} from the skeletal muscle (**A**) and liver (**B**) of 16–20-week-old WT, *BACE1*$^{+/-}$ and *BACE1*$^{-/-}$ mice, 5 and 6 min after insulin injection respectively. The histograms below the immunoblots show the normalized means ± S.E.M of the immunoblots for the skeletal muscle and liver of the indicated genotypes respectively. Results are means ± S.E.M. from 7–19 animals of each genotype. *$P < 0.05$; **$P < 0.01$; ***$P < 0.001$. Molecular mass is given in kDa on the left-hand side.

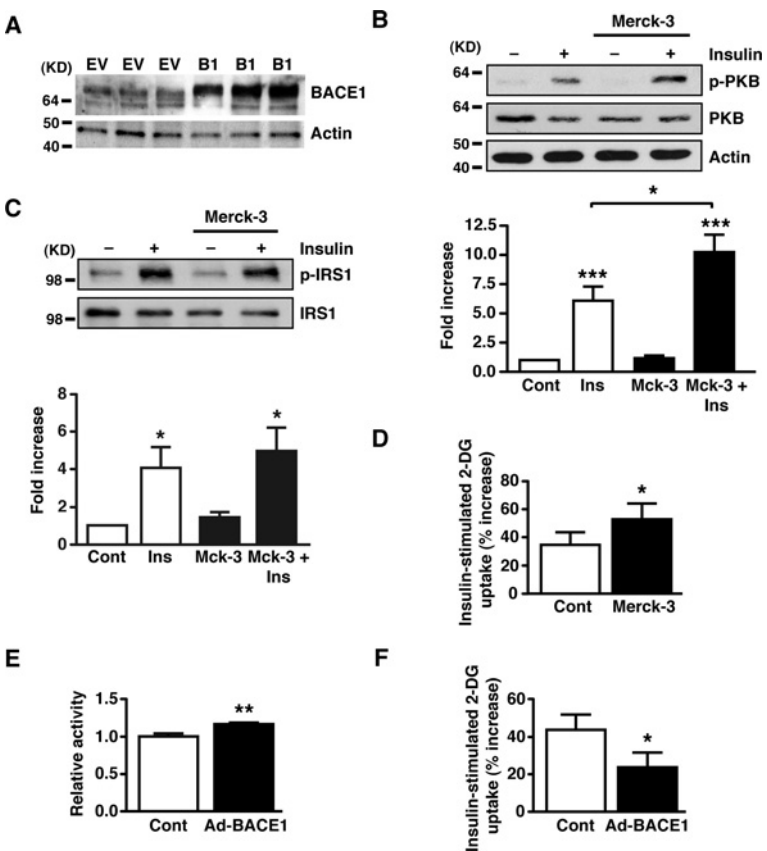

Figure 7 Inhibition of BACE1 increases insulin signalling in C2C12 muscle cells

(**A**) Representative immunoblots showing the presence of BACE1 protein in the mouse C2C12 skeletal muscle cell line under control conditions (EV) and following transfection with adenovirus containing Myc-His-tagged BACE1 (B1). (**B**–**D**) Mouse C2C12 muscle cells were exposed to the BACE1 inhibitor Merck-3 for 24 h, prior to cells being stimulated with saline or insulin for 30 min. (**B**) Representative immunoblots of insulin-stimulated phosphorylation of PKB at Ser^{473} in treated and untreated C2C12 cells. The histograms show the normalized means ± S.E.M. of the immunoblots ($n = 10$). (**C**) Representative immunoblots of IRS-1 and phosphorylated IRS-1 at Tyr^{612} in treated and untreated C2C12 skeletal muscle cells. The histograms show the normalized means ± S.E.M. of the immunoblots ($n = 8$). Molecular mass is given in kDa on the left-hand side. (**D**) Insulin-stimulated 2-deoxyglucose uptake in treated and untreated C2C12 cells, expressed relative to the uptake in the absence of insulin ($n = 11$). (**E**) Relative BACE1 activity in C2C12 cells transfected with empty vector (Cont) or Myc-His-tagged BACE1 ($n = 9$). (**F**) Insulin-stimulated 2-deoxyglucose uptake in C2C12 cells, transfected with empty vector (Cont) or Myc-His-tagged BACE1, expressed relative to uptake in the absence of insulin ($n = 5$). *$P < 0.05$; **$P < 0.01$; ***$P < 0.001$.

measured. Although insulin enhanced phospho-IRS-1 levels in control and Merck-3-treated cells, no difference in phospho-IRS-1 or total IRS levels was observed in Merck-3-treated and untreated muscle cells (Figure 7C), indicating that BACE1 may exert its effect distal to the insulin receptor and its adaptor protein. We next confirmed that altering BACE1 levels and activity in C_2C_{12} muscle cells correlated with changes in glucose uptake. Thus 2-deoxyglucose uptake was measured in C2C12 cells following 24 h of treatment with Merck-3 (50 nM). The presence of the BACE1 inhibitor significantly improved insulin-stimulated glucose uptake in C2C12 myotubes (Figure 7D). Furthermore, when BACE1 was over-expressed in C2C12 muscle cells (Figure 7A), which resulted in a small, but significant, increase in BACE1 activity (Figure 7E), there was a significant reduction in insulin-stimulated 2-deoxyglucose uptake (Figure 7F).

BACE1$^{-/-}$ mice exhibit increased UCP expression

The loss of BACE1 globally in mice results in a lean phenotype, which is associated with reduced fat content, increased energy expenditure and reduced metabolic efficiency, coupled with improved glucose disposal and higher insulin sensitivity. A potential explanation for this phenotype is that removal of BACE1 from highly metabolically active tissues such as BAT and skeletal muscle causes inefficient energy metabolism through modulation of respiratory function (uncoupling). UCPs are considered to be major contributors to diet-induced thermogenesis and decreased energy efficiency [29]. Although the mass of BAT is less in *BACE1*$^{-/-}$ mice (Supplementary Figure S1D) we found no difference in BAT morphology, compared with the WT littermate controls (Figure 8A). However, UCP1 protein levels were increased in BAT from *BACE1*$^{-/-}$ mice compared with their WT littermates when fed on regular chow or the HFD (Figure 8B). It has also been reported that brown adipocytes may be present in WAT (white adipose tissue) and skeletal muscle of rodents [30,31]. As the expression of UCP1 was expected to be much lower in these tissues we performed qRT-PCR (TaqMan®) to measure *UCP1* mRNA levels. The levels of *UCP1* mRNA were extremely low in WAT and skeletal muscle, and these were not consistently altered in *BACE1*$^{-/-}$ mice compared with their WT littermates fed on either regular chow or HFD (results not shown). As skeletal muscle plays a major role in whole-body energy consumption and has the capacity for thermogenesis, we examined this tissue further for evidence of changes driven by the loss of BACE1 and/or the HFD that may link to induction of skeletal muscle thermogenesis. For example, activation of skeletal muscle AMPK (AMP-activated protein kinase) has been linked to skeletal muscle thermogenesis [32] and numerous studies have demonstrated an association between increased expression of UCP2 and UCP3 with uncoupled mitochondrial respiration, protection against fat gain when fed on an HFD and improved muscle insulin sensitivity [33–35]. Skeletal muscle AMPK activity of *BACE1*$^{-/-}$ mice was unaltered in comparison with their WT littermates (Figure 8C). However, *UCP2* and *UCP3* mRNA levels were increased in skeletal muscle of *BACE1*$^{-/-}$ mice relative to their WT littermates (Figures 8D and 8E). Furthermore, exposure to the HFD increased *UCP3* mRNA levels (with a non-significant trend for increased *UCP2* mRNA) in skeletal muscle from WT mice and this effect of the HFD was exaggerated markedly in skeletal muscle of *BACE1*$^{-/-}$ mice (Figures 8D and 8E).

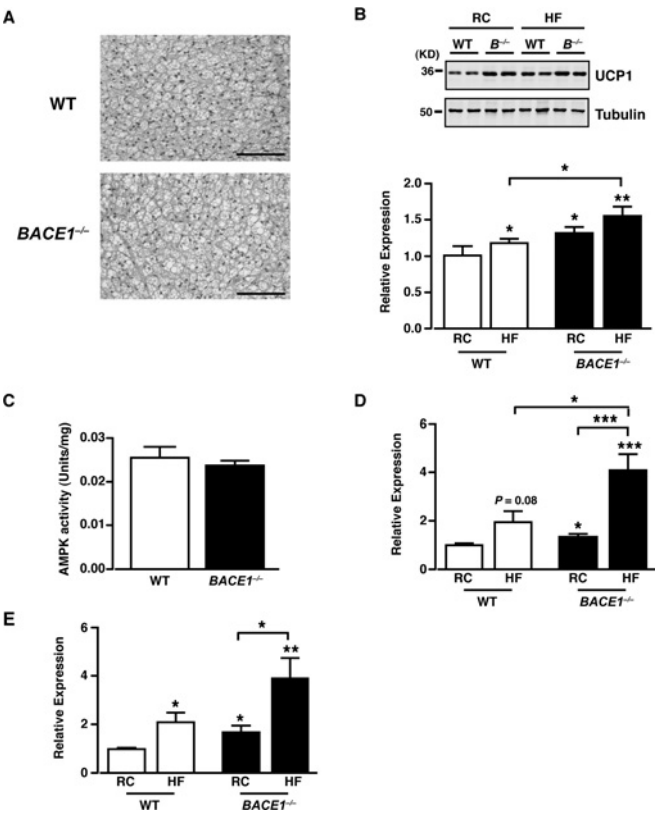

Figure 8 Increased UCP levels in *BACE1*$^{-/-}$ mice

(**A**) H&E (haematoxylin and eosin) staining of BAT from WT and *BACE1*$^{-/-}$ mice fed on a regular chow diet for 20 weeks. Scale bar represents 50 μm. (**B**) Representative immunoblots of UCP1, with tubulin as loading control, from BAT of WT and *BACE1*$^{-/-}$ mice following 20 weeks on the regular chow diet and HFD. The histogram shows mean normalized UCP1 protein expression in WT and *BACE1*$^{-/-}$ BAT on regular and high-fat diet. Results are means $\pm$ S.E.M. for 5–11 animals under each condition. Molecular mass is given in kDa on the left-hand side. (**C**) AMPK activity measured from skeletal muscle of WT and *BACE1*$^{-/-}$ mice following 20 weeks on the regular chow diet. WT, $n = 8$; *BACE1*$^{-/-}$, $n = 8$. Mean normalized *UCP2* mRNA (**D**) and *UCP3* mRNA (**E**) expression in skeletal muscle of WT and *BACE1*$^{-/-}$ mice, following 20 weeks on the regular diet or the HFD. Results are means $\pm$ S.E.M. from 8–14 animals under each condition. $^{*}P < 0.05$; $^{**}P < 0.01$; $^{***}P < 0.001$.

DISCUSSION

Loss or reduction of BACE1 in mice enhanced glucose tolerance and increased insulin-stimulated glucose disposal. HFD-fed WT mice displayed insulin resistance as exemplified by a 4-fold increase in fasted insulin, raised fasted and fed blood glucose levels concomitant with impaired glucose disposal following a bolus injection of glucose. Although *BACE1*$^{-/-}$ mice responded to HFD challenge in a similar manner to WT mice, the absolute levels of glucose, leptin and insulin were all significantly less than for HFD-fed WT mice. Furthermore, HFD-fed *BACE1*$^{-/-}$ mice maintained a significantly improved glucose disposal and insulin sensitivity compared with HFD-fed WT mice. Although regular-chow-fed *BACE1*$^{+/-}$ mice showed no difference in body mass and fasted or fed glucose levels, they had significantly better glucose disposal compared with the control mice. Interestingly, HFD-fed *BACE1*$^{+/-}$ mice revealed initial resistance to increased body mass in association with better whole-body glucose disposal and insulin sensitivity. However, by the end of the HFD, *BACE1*$^{+/-}$ mice had a body mass indistinguishable from HFD-fed WT mice, with evidence of reduced glucose tolerance and insulin sensitivity. A possible explanation was indicated by the observation that BACE1 protein levels and BACE1 activity in skeletal muscle and liver of HFD-fed WT and *BACE1*$^{+/-}$ mice were significantly higher than their lean controls. Thus dietary fat content and/or fat levels may influence whole-body insulin sensitivity and glucose

disposal through modification of BACE1 levels and activity in insulin-sensitive tissues such as skeletal muscle and liver.

These results suggested that BACE1 plays a role in the insulin signalling pathway. Indeed, BACE1 levels increase with age and are greater in brains of AD patients [14,15] and correlates with reduced insulin receptor binding and insulin sensitivity compared with age-matched non-AD controls [8,36,37]. Furthermore, suppression of brain glucose utilization and induction of insulin resistance in rats by intracerebroventricular injection of streptozotocin is associated with pathological and behavioural deficits similar to those observed in AD patients [38,39]. In addition, induction of peripheral insulin resistance in an AD transgenic mouse model reduced brain insulin receptor signalling and increased Aβ content and amyloid plaque burden [9]. Although loss or reduction of BACE1 is insufficient to activate PKB in liver or skeletal muscle at fasted levels of insulin, insulin stimulation increased PKB activation in skeletal muscle and liver of *BACE1*$^{-/-}$ and *BACE1*$^{+/-}$ mice, consistent with a higher insulin sensitivity in these tissues.

Importantly, the enhancement of insulin signalling and glucose uptake was replicated in a skeletal muscle cell line by pharmacological inhibition of BACE1 activity with Merck-3. Furthermore, increasing BACE1 levels and activity in this skeletal muscle cell line resulted in decreased 2-deoxyglucose uptake. These results indicate that the effects of altered BACE1 levels and activity on insulin signal propagation and glucose uptake are likely to be cell autonomous. The effect of BACE1 inhibition in skeletal muscle and liver is commensurate with the reduced glucose levels, enhanced glucose disposal and higher insulin sensitivity of BACE1$^{-/-}$ mice, particularly when exposed to an HFD. At present, the molecular mechanism(s) by which BACE1 reduction alters insulin sensitivity is unclear. BACE1 along with γ-secretase generates Aβ. Extracellular Aβ exists as soluble oligomers [also known as ADDLs (Aβ-derived diffusible ligands], which are toxic to neurons, and are reported to decrease insulin signalling by inhibition of insulin binding to insulin receptors [40] or by ADDL-mediated insulin receptor internalization [41]. It has also been proposed that intracellular Aβ accumulation inhibits insulin receptor signalling by interfering with PKB activation by inhibition of its upstream kinase, PDK (phosphoinositide-dependent kinase) [42]. Our finding that Merck-3 has no effect on insulin-stimulated phospho-IRS-1 (Tyr^{612}) levels does not support a mechanism by which insulin binding or insulin receptor numbers are modified. In contrast, the increased insulin-stimulated phospho-PKB in the liver and muscle cells is consistent with an enhanced PDK–PKB interaction. As multiple substrates for BACE1 exist [16,43] and Aβ targets numerous intracellular signalling pathways [44], it is feasible that tissue- or cell-specific outcomes depend on the relative expression and cellular location of a particular substrate or, if found to be APP-dependent, the ability of Aβ to interact with individual signalling complexes. Clearly, much more detailed analysis of BACE1 activity and substrate sensitivity in individual tissues and cells is required.

BACE1$^{-/-}$ mice are leaner with less body fat than the WT controls, a phenotype they maintained throughout the study period (and which was present in animals more than 21 months old; results not shown). In contrast, *BACE1*$^{+/-}$ mice exhibited growth curves and body mass equivalent to the WT controls. Exposure to an HFD resulted in WT and *BACE1*$^{-/-}$ mice gaining body mass, although the *BACE1*$^{-/-}$ mice remained leaner throughout the HFD period. However, *BACE1*$^{+/-}$ mice, although maintaining a lower body mass for the first few weeks of the HFD, eventually gained mass so that by the end of the 20 weeks of HFD they were the same mass as their WT littermates. The increase in body mass in WT and *BACE1*$^{+/-}$ mice was associated with increased tissue BACE1 levels and activity. Clearly, further studies are required to determine whether there is a causal relationship between BACE1 activity and susceptibility to mass gain and loss of glucose homoeostasis. The absolute amount of regular chow consumed by *BACE1*$^{-/-}$ mice did not differ from WT mice and on the HFD was only marginally less than WT mice. However, when adjusted for body mass, *BACE1*$^{-/-}$ mice consumed more than the WT mice on either diet, indicating they are less metabolically efficient. *BACE1*$^{-/-}$ mice have reduced levels of leptin when fed on regular chow and the HFD, consistent with their lower levels of body fat, which may explain the higher relative food intake of *BACE1*$^{-/-}$ mice. *BACE1*$^{-/-}$ mice exhibited no difference in blood lipid levels or stool mass, although they had less lipid in their stools compared with the WT mice. These results, along with the decreased adiposity and resistance to diet-induced obesity, suggested that *BACE1*$^{-/-}$ mice exhibit higher energy expenditure.

Indeed, *BACE1*$^{-/-}$ mice had a higher RMR with no change in serum T_4 levels compared with the controls, indicating that thyroid-hormone-mediated changes in metabolism are unlikely to explain this outcome. The increased RMR was detected after appropriate normalization for the effects of body mass and sex using ANCOVA. Normalization of energy expenditure in relation to body mass is a long-standing issue in the interpretation of energy expenditure data [45,46] and ANCOVA is the most appropriate approach to overcome such problems [47]. As our measurements only addressed differences in resting metabolism, although energy balance is a consequence of resting, activity and thermoregulatory demands, more detailed studies of energy regulation by *BACE1*$^{-/-}$ mice are clearly required. Nevertheless, we were unable to detect any effect of genotype on locomotor activity in agreement with a previous study of this line of *BACE1*$^{-/-}$ mice [21]. Their higher metabolic rate was accompanied by an increased RQ, indicating that *BACE1*$^{-/-}$ mice at rest utilized a higher carbohydrate-to-fat ratio than did the WT mice. This effect was unexpected since mice that are resistant to fat deposition frequently show increased fat oxidation rates. The elevated levels of carbohydrate oxidation, however, may reflect their enhanced capacity to dispose of glucose.

One potential mechanism that could explain the metabolic inefficiency and increased energy expenditure of *BACE1*$^{-/-}$ mice is increased thermogenesis. BAT and skeletal muscle are important sites for the induction of thermogenesis with the UCPs intimately involved in this process. Indeed loss of UCP1 in mice results in an increased susceptibility to diet-induced obesity with age [48], and ectopic expression of UCP1 via the presence of brown adipocytes in skeletal muscle protects mice from diet-induced mass gain [31]. We found that UCP1 protein levels are increased in BAT of *BACE1*$^{-/-}$ mice, an outcome enhanced by the HFD, indicative of raised thermogenesis and energy expenditure. Although we could not detect any increase in *UCP1* mRNA or protein levels in WAT or skeletal muscle of *BACE1*$^{-/-}$ mice, we observed increased levels of *UCP2* and *UCP3* mRNA in skeletal muscle of *BACE1*$^{-/-}$ mice, which were enhanced by high-fat feeding. The exact physiological roles for UCP2 and UCP3 are presently unclear, with their role in adaptive thermogenesis questioned and alternative functions proposed, including acting as regulators of muscle lipid metabolism and reactive oxygen species production [49]. Importantly within the context of our results and irrespective of exact mechanism, it has been shown that decreased expression of UCP3 in skeletal muscle is associated with insulin insensitivity, whereas UCP3 overexpression improves muscle insulin sensitivity and protects against diet-induced obesity [33–35]. A mechanism that may, at least in part, underlie the increased expression of UCPs is that loss of BACE1 centrally could result in an increased sympathetic drive

to peripheral tissues. Indeed increased release of noradrenaline from sympathetic nerve terminals causes increased activity of BAT β_3-adrenoceptors, which signals via PKA (protein kinase A) to drive expression of UCP1 [50].

Taken together, the results of the present study indicate that deletion or reduction of BACE1 not only renders mice lean and insulin-sensitive when fed on a regular chow diet, but also causes them to be, at least partially, protected against the metabolic derangement caused by chronic exposure to nutrient excess, in the form of an HFD. These actions may be mediated, at least in part, by increased expression of uncoupling proteins in BAT and skeletal muscle, resulting in increased thermogenesis and improved insulin sensitivity. Consequently, strategies to maintain reduced BACE1 levels and activity may be sufficient to ameliorate the adverse metabolic consequences of an HFD, particularly in individuals more susceptible to Type 2 diabetes.

AUTHOR CONTRIBUTION

Paul Meakin researched the data, contributed to the discussion and reviewed/edited the paper prior to submission. Alex Harper researched the data and contributed to the discussion. Lee Hamilton, Jennifer Gallagher, Alison McNeilly, Laura Burgess, Lobke Vaanholt, Kirsten Bannon and Judy Latcham researched the data. Ishrut Hussain reviewed/edited the paper prior to submission. John Speakman researched the data, contributed to the discussion and reviewed/edited the paper prior to submission. David Howlett contributed to the discussion and reviewed/edited paper prior to submission. Michael Ashford contributed to the discussion, wrote the paper and reviewed/edited the paper prior to submission.

ACKNOWLEDGEMENTS

We are grateful to GlaxoSmithKline for providing the *BACE1*$^{-/-}$ mouse line and the Myc-His-tagged BACE1.

FUNDING

This work was supported by the Wellcome Trust [grant numbers 068692 and 086989], Diabetes U.K., GlaxoSmithKline, the Nuffield Foundation and a Biotechnology and Biological Sciences Research Council CASE Award (with GlaxoSmithKline) studentship (to P.M.).

REFERENCES

1 Biessels, G. J., Staekenborg, S., Brunner, E., Brayne, C. and Scheltens, P. (2006) Risk of dementia in diabetes mellitus: a systematic review. Lancet Neurol. **5**, 64–74
2 Janson, J., Laedtke, T., Parisi, J. E., O'Brien, P., Petersen, R. C. and Butler, P. C. (2004) Increased risk of Type 2 diabetes in Alzheimer disease. Diabetes **53**, 474–481
3 Luchsinger, J. A. and Gustafson, D. R. (2009) Adiposity, Type 2 diabetes and Alzheimer's disease. J. Alzheimer's Dis. **16**, 693–704
4 Hassing, L. B., Dahl, A. K., Thorvaldsson, V., Berg, S., Gatz, M., Pedersen, N. L. and Johansson, B. (2009) Overweight in midlife and risk of dementia: a 40-year follow-up study. Int. J. Obes. **33**, 893–898
5 Craft, S., Peskind, E., Schwartz, M. W., Schellenberg, G. D., Raskind, M. and Porte, Jr, D. (1998) Cerebrospinal fluid and plasma insulin levels in Alzheimer's disease: relationship to severity of dementia and apolipoprotein E genotype. Neurology **50**, 164–168
6 Rapoport, S. I. (1999) Functional brain imaging in the resting state and during activation in Alzheimer's disease. Implications for disease mechanisms involving oxidative phosphorylation. Ann. N.Y. Acad. Sci. **893**, 138–153
7 Frölich, L., Blum-Degen, D., Bernstein, H. G., Engelsberger, S., Humrich, J., Laufer, S., Muschner, D., Thalheimer, A., Türk, A., Hoyer, S. et al. (1998) Brain insulin and insulin receptors in aging and sporadic Alzheimer's disease. J. Neural Transm. **105**, 423–438
8 Steen, E., Terry, B. M., Rivera, E. J., Cannon, J. L., Neely, T. R., Tavares, R., Xu, X. J., Wands, J. R. and de la Monte, S. M. (2005) Impaired insulin and insulin-like growth factor expression and signalling mechanisms in Alzheimer's disease: is this Type 3 diabetes? J. Alzheimer's Dis. **7**, 63–80
9 Ho, L., Qin, W., Pompl, P. N., Xiang, Z., Wang, J., Zhao, Z., Peng, Y., Cambareri, G., Rocher, A., Mobbs, C. V. et al. (2004) Diet-induced insulin resistance promotes amyloidosis in a transgenic mouse model of Alzheimer's disease. FASEB J. **18**, 902–904
10 LaFerla, F. M., Green, K. N. and Oddo, S. (2007) Intracellular amyloid-β in Alzheimer's disease. Nat. Rev. Neurosci. **8**, 499–509
11 Cai, H., Wang, Y., McCarthy, D., Wen, H., Borchelt, D. R., Price, D. L. and Wong, P. C. (2001) BACE1 is the major β-secretase for generation of Aβ peptides by neurons. Nat. Neurosci. **4**, 233–234
12 Luo, Y., Bolon, B., Kahn, S., Bennett, B. D., Babu-Khan, S., Denis, P., Fan, W., Kha, H., Zhang, J., Gong, Y. et al. (2001) Mice deficient in BACE1, the Alzheimer's β-secretase, have normal phenotype and abolished β-amyloid generation. Nat. Neurosci. **4**, 231–232
13 Roberds, S. L., Anderson, J., Basi, G., Bienkowski, M. J., Branstetter, D. G., Chen, K. S., Freedman, S. B., Frigon, N. L., Games, D., Hu, K. et al. (2001) BACE knockout mice are healthy despite lacking the primary β-secretase activity in brain: implications for Alzheimer's disease therapeutics. Hum. Mol. Genet. **10**, 1317–1324
14 Fukumoto, H., Cheung, B. S., Hyman, B. T. and Irizarry, M. C. (2002) β-Secretase protein and activity are increased in the neocortex in Alzheimer disease. Arch. Neurol. **59**, 1381–1389
15 Li, R., Lindholm, K., Yang, L. B., Yue, X., Citron, M., Yan, R., Beach, T., Sue, L., Sabbagh, M., Cai, H. et al. (2004) Amyloid β peptide load is correlated with increased β-secretase activity in sporadic Alzheimer's disease patients. Proc. Natl. Acad. Sci. U.S.A. **101**, 3632–3637
16 Cole, S. L. and Vassar, R. (2007) The Alzheimer's disease β-secretase enzyme, BACE1. Mol. Neurodegener. **2**, 22
17 Vassar, R., Bennett, B. D., Babu-Khan, S., Kahn, S., Mendiaz, E. A., Denis, P., Teplow, D. B., Ross, S., Amarante, P., Loeloff, R. et al. (1999) β-Secretase cleavage of Alzheimer's amyloid precursor protein by the transmembrane aspartic protease BACE. Science **286**, 735–741
18 Vattemi, G., Engel, W. K., McFerrin, J., Pastorino, L., Buxbaum, J. D. and Askansas, V. (2003) BACE1 and BACE2 in pathologic and normal human muscle. Exp. Neurol. **179**, 150–158
19 Huse, J. T., Byant, D., Yang, Y., Pijak, D. S., D'Souza, I., Lah, J. J., Lee, V. M., Doms, R. W. and Cook, D. G. (2003) Endoproteolysis of β-secretase (β site amyloid precursor protein-cleaving enzyme) within its catalytic domain. A potential mechanism for regulation. J. Biol. Chem. **278**, 17141–17149
20 Kobayashi, D., Zeller, M., Cole, T., Buttini, M., McConlogue, L., Sinha, S., Freedman, S., Morris, R. G. and Chen, K. S. (2008) *BACE1* gene deletion: impact on behavioural function in a model of Alzheimer's disease. Neurobiol. Aging **29**, 861–873
21 Harrison, S. M., Harper, A. J., Hawkins, J., Duddy, G., Grau, E., Pugh, P. L., Winter, P. H., Shilliam, C. S., Hughes, Z. A., Dawson, L. A. et al. (2003) BACE1 (β-secretase) transgenic and knockout mice: identification of neurochemical deficits and behavioural changes. Mol. Cell. Neurosci. **24**, 646–655
22 Folch, J., Lees, M. and Sloane-Stanley, G. H. (1957) A simple method for the isolation and purification of total lipids from animal tissues. J. Biol. Chem. **226**, 497–509
23 Selman, C., Lumsden, S., Bünger, L., Hill, W. G. and Speakman, J. R. (2001) Resting metabolic rate and morphology in mice (*Mus musculus*) selected for high and low food intake. J. Exp. Biol. **204**, 777–784
24 Mirshamsi, S., Laidlaw, H. A., Ning, K., Anderson, E., Burgess, L. A., Gray, A., Sutherland, C. and Ashford, M. L. (2004) Leptin and insulin stimulation of signaling pathways in arcuate nucleus neurons: PI3K dependent actin reorganization and K_{ATP} channel activation. BMC Neurosci. **5**, 54
25 Dominguez, D., Tournoy, J., Hartmann, D., Huth, T., Cryns, K., Deforce, S., Serneels, L., Camacho, I. E., Marjaux, E., Craessaerts, K. et al. (2005) Phenotypic and biochemical analyses of BACE1- and BACE2-deficient mice. J. Biol. Chem. **280**, 30797–30806
26 Burcelin, R., Crivelli, V., Dacosta, A., Roy-Tirelli, A. and Thorens, B. (2002) Heterogeneous metabolic adaptation of C57BL/6J mice to high-fat diet. Am. J. Physiol. Endocrinol. Metab. **282**, E834–E842
27 Sankaranarayanan, S., Price, E. A., Wu, G., Crouthamel, M. C., Shi, X. P., Tugusheva, K., Tyler, K. X., Kahana, J., Ellis, J., Jin, L. et al. (2008) *In vivo* β-secretase 1 inhibition leads to brain Aβ lowering and increased α-secretase processing of amyloid precursor protein without effect on neuregulin-1. J. Pharmacol. Exp. Ther. **324**, 957–969
28 Pietrak, B. L., Crouthamel, M. C., Tugusheva, K., Lineberger, J. E., Xu, M., DiMuzio, J. M., Steele, T., Espeseth, A. S., Stachel, S. J., Coburn, C. A. et al. (2005) Biochemical and cell-based assays for characterization of BACE-1 inhibitors. Anal. Biochem. **342**, 144–151
29 Cioffi, F., Senese, R., deLange, P., Goglia, F., Lanni, A. and Lombardi, A. (2009) Uncoupling proteins: a complex journey to function discovery. BioFactors **35**, 417–428
30 Fromme, T. and Klingenspor, M. (2011) Uncoupling protein 1 expression and high-fat diets. Am. J. Physiol. Regul. Integr. Comp. Physiol. **300**, R1–R8
31 Almind, K., Manieri, M., Sivitz, W. I., Cinti, S. and Khan, C. R. (2007) Ectopic brown adipose tissue in muscle provides a mechanism for differences in risk of metabolic syndrome in mice. Proc. Natl. Acad. Sci. U.S.A. **104**, 2366–2371
32 Kus, V., Prazak, T., Brauner, P., Hensler, M., Kuda, O., Flachs, P., Janovska, P., Medrikova, D., Rossmeisl, M., Jilkova, Z. et al. (2008) Induction of muscle thermogenesis by high-fat diet in mice: association with obesity resistance. Am. J. Physiol. Endocrinol. Metab. **295**, E356–E367

33 Mensink, M., Hesselink, M. K., Borghouts, L. B., Keizer, H., Moonen-Kornips, E., Schaart, G., Blaak, E. E. and Schrauwen, P. (2007) Skeletal muscle uncoupling protein-3 restores upon intervention in the prediabetic and diabetic state: implications for diabetes pathogenesis. Diabetes Obes. Metab. **9**, 594–596
34 Tiraby, C., Tavernier, G., Capel, F., Mairal, A., Crampes, F., Rami, J., Pujol, C., Boutin, J. A. and Langin, D. (2007) Resistance to high-fat-diet-induced obesity and sexual dimorphism in the metabolic responses of transgenic mice with moderate uncoupling protein 3 overexpression in glycolytic skeletal muscles. Diabetologia **50**, 2190–2199
35 Choi, C. S., Fillmore, J. J., Kim, J. K., Liu, Z-X., Kim, S., Collier, E. F., Kulkarni, A., Distefano, A., Hwang, Y-J., Khan, M. et al. (2007) Overexpression of uncoupling protein 3 in skeletal muscle protects against fat-induced insulin resistance. J. Clin. Invest. **117**, 1995–2003
36 Rivera, E. J., Goldin, A., Fulmer, N., Tavares, R., Wands, J. R. and de la Monte, S. M. (2005) Insulin and insulin-like growth factor expression and function deteriorate with progression of Alzheimer's disease: link to brain reductions in acetylcholine. J. Alzheimer's Dis. **8**, 247–268
37 Craft, S. (2007) Insulin resistance and Alzheimer's disease pathogenesis: potential mechanisms and implications for treatment. Curr. Alzheimer Res. **4**, 1 47–152
38 de la Monte, S. M., Tong, M., Lester-Coll, N., Plater, Jr, M. and Wands, J. R. (2006) Therapeutic rescue of neurodegeneration in experimental Type 3 diabetes: relevance to Alzheimer's disease. J. Alzheimer's Dis. **10**, 89–109
39 de la Monte, S. M. and Wands, J. R. (2008) Alzheimer's disease is Type 3 diabetes-evidence reviewed. J. Diabetes Sci. Technol. **2**, 1101–1113
40 Xie, L., Helmerhorst, E., Taddei, K., Plewright, B., Van Bronswijk, W. and Martins, R (2002) Alzheimer's β-amyloid peptides compete for insulin binding to the insulin receptor. J. Neurosci. **22**, RC221
41 De Felice, F. G., Vieira, M. N., Bomfim, T. R., Decker, H., Velasco, P. T., Lambert, M. P., Viola, K. L., Zhao, W. Q., Ferreira, S. T. and Klein, W.L (2009) Protection of synapses against Alzheimer's-linked toxins: insulin signalling prevents the pathogenic binding of Aβ oligomers. Proc. Natl. Acad. Sci. U.S.A. **106**, 1971–1976
42 Lee, H.-K., Kumar, P., Fu, Q., Rosen, K. M. and Querfurth, H. W. (2009) The insulin/Akt signalling pathway is targeted by intracellular β-amyloid. Mol. Biol. Cell **20**, 1533–1544
43 Vassar, R., Kovacs, D. M., Yan, R. and Wong, P. C. (2009) The β-secretase enzyme BACE in health and Alzheimer's disease: regulation, cell biology, function and therapeutic potential. J. Neurosci. **29**, 12787–12794
44 Balleza-Tapia, H. and Peña, F. (2009) Pharmacology of the intracellular pathways activated by amyloid β protein. Mini Rev. Med. Chem. **9**, 724–740
45 Butler, A. A. and Kozak, L. P. (2010) A recurring problem with the analysis of energy expenditure in genetic models expressing lean and obese phenotypes. Diabetes **59**, 323–329
46 Speakman, J. R. (2010) FTO effect on energy demand versus food intake. Nature **464**, E1
47 Arch, J.R.S., Hislop, D., Wang, S.J.Y. and Speakman, J. R. (2006) Some mathematical and technical issues in the measurement and interpretation of open-circuit indirect calorimetry in small animals. Int. J. Obes. **30**, 1322–1331
48 Kontani, Y., Wang, Y., Kimura, K., Inokuma, K. I., Saito, M., Suzuki-Miura, T., Wang, Z., Sato, Y., Mori, N. and Yamashita, H. (2005) UCP1 deficiency increases susceptibility to diet-induced obesity with age. Aging Cell **4**, 147–155
49 Azzu, V. and Brand, M. D. (2010) The on-off switches of the mitochondrial uncoupling proteins. Trends Biochem. Sci. **35**, 298–307
50 Cannon, B. and Nedergaard, J. (2004) Brown adipose tissue: function and physiological significance. Physiol. Rev. **84**, 277–359

Received 21 March 2011/18 August 2011; accepted 31 August 2011
Published as BJ Immediate Publication 31 August 2011, doi:10.1042/BJ20110512

Biochem. J. (2012) **441**, 285–296 (Printed in Great Britain) doi:10.1042/BJ20110512

online data

SUPPLEMENTARY ONLINE DATA

Reduction in BACE1 decreases body weight, protects against diet-induced obesity and enhances insulin sensitivity in mice

Paul J. MEAKIN*[1], Alex J. HARPER†[1,2], D. Lee HAMILTON*, Jennifer GALLAGHER*, Alison D. McNEILLY‡, Laura A. BURGESS*, Lobke M. VAANHOLT§, Kirsten A. BANNON*, Judy LATCHAM†, Ishrut HUSSAIN†[3], John R. SPEAKMAN§, David R. HOWLETT†[4] and Michael L.J. ASHFORD*[5]

*Division of Cardiovascular and Diabetes Medicine, Medical Research Institute, Ninewells Hospital and Medical School, University of Dundee, Dundee DD1 9SY, Scotland, U.K., †Neuroscience Centre of Excellence for Drug Discovery, GlaxoSmithKline R&D, New Frontiers Science Park, Harlow CM19 5AW, U.K., ‡Division of Neuroscience, University of Dundee, Medical Research Institute, Dundee DD1 9SY, Scotland, U.K., and §Aberdeen Centre for Energy Regulation and Obesity, Institute of Biological and Environmental Sciences, University of Aberdeen, Aberdeen AB24 2TZ, Scotland, U.K.

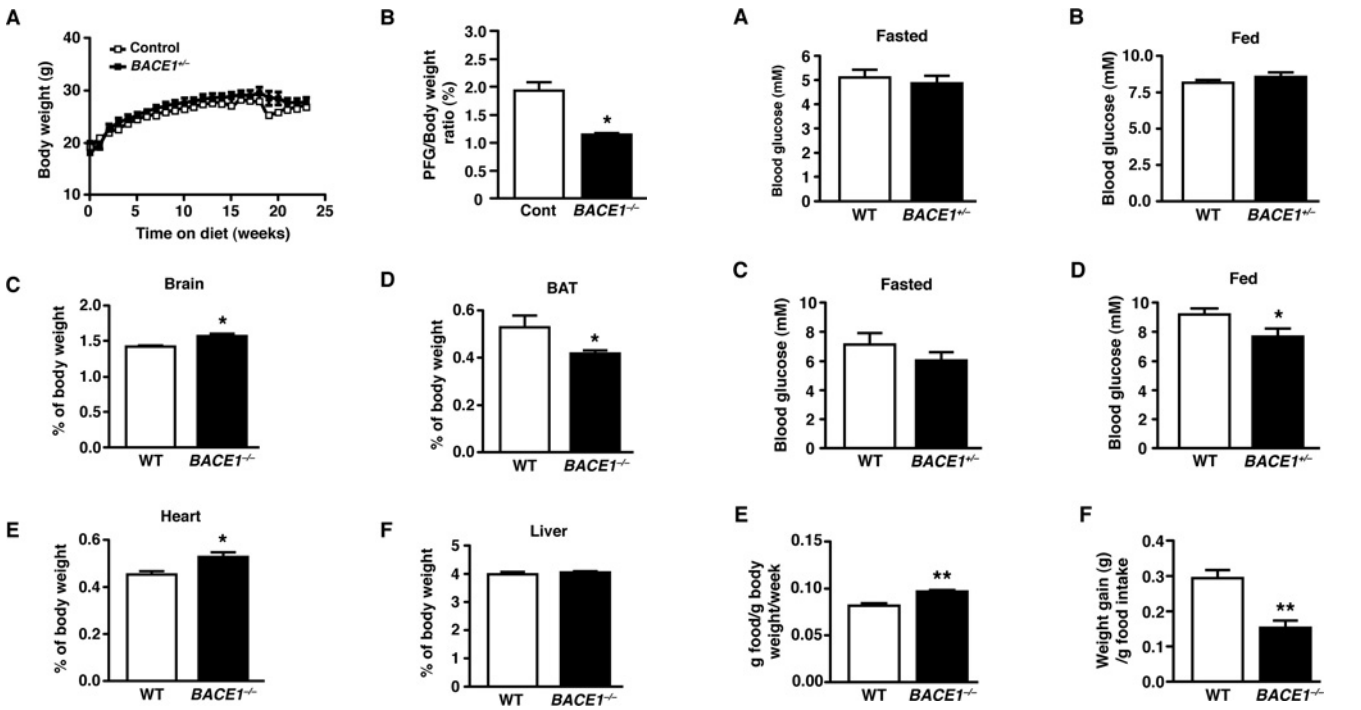

Figure S1 Body mass of BACE1$^{+/-}$, and tissue mass of BACE1$^{-/-}$ mice compared with their WT littermates

(**A**) Body mass curves of age-matched WT littermates with *BACE1*$^{+/-}$ mice fed on a regular chow diet and monitored over a period of 24 weeks from 9 weeks of age. Results are means ± S.E.M. from 7–8 animals of each genotype. The relative masses (expressed as the percentage of total body mass) of perigenital fat (**B**), brain (**C**), BAT (**D**), heart (**E**) and liver (**F**) for WT and *BACE1*$^{-/-}$ mice are shown. Results are means ± S.E.M. from 5–7 animals of each genotype. *$P < 0.05$.

Figure S2 Comparison of the effects of diet on WT, BACE1$^{+/-}$ and BACE1$^{-/-}$ mice

Fasted (**A**) and fed (**B**) blood glucose levels of 8-month-old male mice of the indicated genotypes fed on a regular chow diet ($n = 6$–10). Fasted (**C**) and fed (**D**) blood glucose levels of 10-month-old mice of the indicated genotypes fed on an HFD for 20 weeks. (**E**) Food intake per mouse per week normalized by body mass (relative food intake) for mice of the indicated genotypes fed on an HFD. (**F**) BACE$^{-/-}$ mice on a HFD have decreased feed efficiency compared with the WT controls. Results are means ± S.E.M. from 11–14 animals of each genotype. **$P < 0.01$;*$P < 0.05$.

[1] These authors contributed equally to this work.
[2] Present address: Lilly Research Laboratories, Eli Lilly & Co., Erlwood Manor, Sunninghill Road, Windlesham, GU20 6PH. U.K.
[3] Present address: Merck Serono S.A., Chemin des Mines 9, 1202 Geneva, Switzerland
[4] Present address: Wolfson Centre for Age-Related Diseases, King's College London, London SE1 1UL, U.K.
[5] To whom correspondence may be addressed (email m.l.j.ashford@dundee.ac.uk).

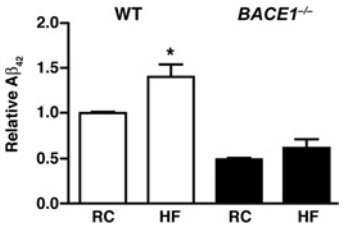

Figure S3 A 20-week HFD was shown to increase levels of A$\beta_{x\text{-}42}$ in the cerebral cortices of WT mice, but not *BACE1*$^{-/-}$ mice

Results from an ELISA showing the level of A$\beta_{x\text{-}42}$ (normalized to mean WT, normal chow diet amount) in the cerebral cortices of WT and BACE$^{-/-}$ mice fed on a regular chow (RC) diet or an HFD. WT, $n = 5$; BACE$^{-/-}$, $n = 6$. Results are means $\pm$ S.E.M. *$P < 0.05$.

Received 21 March 2011/18 August 2011; accepted 31 August 2011
Published as BJ Immediate Publication 31 August 2011, doi:10.1042/BJ20110512